

Tmrees, EURACA, 13 to 16 April 2020, Athens, Greece

# Phenol-derived products from fast pyrolysis of organosolv lignin

Kanit Soongprasit<sup>a</sup>, Viboon Sricharoenchaikul<sup>b</sup>, Duangduen Atong<sup>a,\*</sup><sup>a</sup> National Metal and Materials Technology Center, 114 Thailand Science Park, Paholyothin Rd., Klong Nueng, Klongluang, Pathumthani 12120, Thailand<sup>b</sup> Department of Environmental Engineering, Faculty of Engineering, Chulalongkorn University, Pathumwan, Bangkok 10330, Thailand

Received 2 August 2020; accepted 30 August 2020

## Abstract

Lignin is the largest aromatic bio-polymer feedstock with a huge potential of being refined for aromatic chemical platform and building block. Organosolv process for lignin extraction has a low impact on the environment due to its low chemical requirement, the absence of sulfur, and as it is more practical for chemical recovery. Therefore, refinement of extracted lignin to valuable molecular compounds such as purified lignin and its derivative is the key success for biorefinery industry. In this study, sugarcane bagasse from a local sugar manufacturer in Thailand, noted as BG-lignin, was selected as feedstock for lignin extraction using ethanol and water. The chemical composition of this lignin was slightly different than that of commercially available organosolv lignin, noted as Comm-OS-lignin, in that BG-lignin has more combustible constituents (volatile organic compounds and fixed carbon) of 96.14% and low ash content of 0.09%. The chemical structure of BG-lignin contains a higher number of aliphatic hydrocarbon and aliphatic hydroxy side chains than Comm-OS-lignin, as confirmed by the FT-IR and <sup>1</sup>H-NMR analyses. The study on fast pyrolysis of lignin, using Py-GCMS technique, found 2, 3-dihydrobenzofuran as a major constituent at any tested pyrolysis temperature. H-unit, G-unit, and S-unit are distributed in resemble fraction with a *H/G/S* ratio of 1/1/0.7 and 0.8/1/1 for Comm-OS-lignin and BG-lignin, respectively, at pyrolysis temperature of 400–600 °C, except for H-unit which was enhanced at 700 °C to 28.82% of Comm-OS-lignin and 29.66% of BG-lignin. At a temperature of 400–600 °C, phenolic selectivity of pyrolyzed products, mainly methoxy phenol (Ph-OCH<sub>3</sub>) and alkylated phenol (R-Ph-OCH<sub>3</sub>), was done. A higher pyrolysis temperature of 700 °C led to the elimination of aromatic side group and is more favorable in alkyl phenol (R-Ph) and phenol selectivity. However, reduction of the phenolic compound was observed with a higher temperature due to thermal fragmentation of the C–C linkage in the aromatic structure. Products selectivity related to lignin feedstock and pyrolysis temperature could be applied as a conceptual guideline for conducting further study of chemical upgrading process to obtain high-value biochemical products.

© 2020 The Author(s). Published by Elsevier Ltd. This is an open access article under the CC BY-NC-ND license (<http://creativecommons.org/licenses/by-nc-nd/4.0/>).

Peer-review under responsibility of the scientific committee of the Tmrees, EURACA, 2020.

**Keywords:** Phenol; Lignin; Organosolv; Fast pyrolysis; Delignification; Biorefinery

\* Corresponding author.

E-mail address: [duangdua@mtec.or.th](mailto:duangdua@mtec.or.th) (D. Atong).

<https://doi.org/10.1016/j.egy.2020.08.040>

2352-4847/© 2020 The Author(s). Published by Elsevier Ltd. This is an open access article under the CC BY-NC-ND license (<http://creativecommons.org/licenses/by-nc-nd/4.0/>).

Peer-review under responsibility of the scientific committee of the Tmrees, EURACA, 2020.

## Nomenclature

Comm-OS-lignin	Commercial organosolv lignin
BG-lignin	Bagasse lignin
EtOH	Ethanol
Py	Pyrolyzer
GC	Gas chromatography
MS	Mass spectrophotometer
H-unit	p-Hydroxyphenyl unit
G-unit	Guaiacyl unit
S-unit	Syringyl unit
O-comp	Oxygen containing compound
OR-Ph-OCH <sub>3</sub>	Oxygenated-alkyl methoxy phenol
R-Ph-OCH <sub>3</sub>	Alkyl methoxy phenol
Ph-OCH <sub>3</sub>	Methoxy phenol
R-Ph	Alkyl phenol
Ph	Phenol

## 1. Introduction

Lignin is one of the most abundant aromatic bio-polymer feedstock, found in around 15%–30% of plants in terms of dry weight and 40% in terms of energy. Although it has high potential, it is still underutilized as a bio-based chemical and biofuel compared to cellulose and hemicellulose [1,2]. Kraft and soda delignification process is usually used in pulp and paper plants to extract cellulose as pulp from lignocellulosic materials while generating lignin-enriched black liquor as a byproduct of more than 50 million tons per year [3]. Most of the black liquor is concentrated through multi-staged evaporation and fed to a special boiler for heat and power generation as well as pulping chemical recovery. Therefore, transformation of lignin in lignocellulosic feedstock into high value bio-chemicals is being widely considered in order to replace petroleum-based chemicals. A large-scale utilization of lignin in relevant industries will significantly promote biorefinery competitiveness. Wang et al. [4] stated that the improvement of the extraction efficiency with 20% of the global lignin in biomass would further boost the total revenue to 100 USD/ton as a result of reduced feedstock cost.

Lignin is a three-dimensional cross-linked polymer with a complex structure that is composed of three monolignol or phenolpropanoid units, which are formed as a result of photosynthesis in plants. These units include p-hydroxyphenyl (H-unit), guaiacyl (G-unit), and syringyl (S-unit), which are derived from p-coumaryl alcohol, coniferyl alcohol, and sinapyl alcohol, respectively, by mostly coupling together with ether linkage (C–O) and C–C linkage [2,3,5,6]. Ether linkage is mainly found in lignin structure, especially in  $\beta$ -O-4, which was reported to be about 50%–60% in biomass and varied with the plant type and location [3]. Examples of other linkages between lignin monomer unit are 5-5,  $\beta$ -5, 4-O-5, and  $\beta$ - $\beta$ . Due to various linkages and bonding constituents in lignin, exact structures of hardwood, softwood, and herbaceous plants are still not definite. Moreover, as a result of the complexity and stereoregularity of lignin structure, isolation and purification of lignin to targeted substance can be laborious and challenging [7–9].

Implementation of biorefinery of lignin from residual and nonedible biomass is one of the key strategies of encouraging BCG economy (bio-economy, circular economy, and green economy) which had been launched in many countries. Valorization of lignin to phenol-derived molecular such as vanillin and BTX is promising solution to overcome the limitation of economy and competitiveness that are inferior to fossil feedstock. Rigorous oxidation of lignin during delignification irreparably altered its structure and consequently, greatly limited its scope of being subsequently upgraded to chemical platform and high value reactant [10]. Thus, the biorefinery process that focuses on lignin with its chemical structure closely to a native lignin, called “*lignin-first*”, is notably attractive.

Delignification or lignin isolation process strongly effects the chemical structure, molecular weight, functional group, thermal properties, and impurities. The so-called technical lignin from the kraft process is abundant, as this

is a major pulping operation of the pulp and paper industry. The reactions that occur during delignification result in bonded sulfur, mainly thiols [11] and cleavage of ether linkage, demethoxylation reaction, and repolymerization by C–C linkage. The soda process is different from kraft pulping in that only NaOH is used as cooking medium in the former, whereas in the latter, Na<sub>2</sub>S is also added. The technical lignin from the soda process is quite similar to the native lignin used in the kraft process and could be used without purification [5]. For organosolv process, organic solvents, such as ethanol, methanol, acetic acid, and medium, usually water, were used to separate lignin from cellulose and hemicellulose. The obtained lignin from this process is highly pure and most suitable to be used for further chemical modification and functionalization without purification.

In order to achieve economic growth in biorefinery initiative, strategy of lignin valorization is divided into two ways [12]. First, ensuring modification and functionalization of lignin macromolecule to improve compatibility with and performance of the copolymer, nanoparticles, composite, adhesive, carbon fiber, and resin. This strategy is to directly utilize lignin without subjecting it to chemical conversion process. Second, lignin depolymerization to a highly value-added biochemical in order to replace petroleum-derived building block and chemical platform through a thermochemical conversion such as pyrolysis and gasification. Lignin degradation by pyrolysis in the absence of oxygen atmosphere at 400–500 °C leads to the production of phenolic compound and other chemicals [13]. Pyrolysis pathway of lignin is complex and highly dependent on the operating conditions such as temperature, biomass, heating, and additives [14].

Son et al. [15] studied the phenolic production from organosolv lignin which is extracted from four different biomasses: agricultural waste, softwood, hardwood, and grass. They are strongly related to the distribution of monolignol and pyrolysis behavior. The presence of bulky methoxy group inhibited the attraction of ether bonding to catalysts surface that resulted in repolymerization of lignin due to C–C and  $\beta$ – $\beta$  formation. In Huang et al. [16], pyrolysis of isolated lignin from corn cob acid hydrolysis residue (CAHL) by enzymatic acid hydrolysis method was studied. Thermal degradation of CAHL occurred in wide range between 180–850 °C with two major decomposition taking place at 237 °C and 340 °C. Interpretation data from the Py-GCMS analysis reported the dominant presence of chemical compounds, guaiacol and syringol, which are generated from cracking of arylglycero *l*- $\beta$ -*e* ther ( $\beta$ -O-4) linkage. Kim et al. [17] examined the structural features and thermal decomposition of four types of lignin: milled wood lignin (ML), organosolv lignin (OL), ionic liquid lignin (IL), and Klason lignin (KL). The dominant nature of condensation reaction of phenolic hydroxyl results in highly condensed OL and KL structure. The number of  $\beta$ -O-4 in lignin polymer strongly effected the thermal stability of the isolated lignin. The oxygen contained in the side chain of lignin is quite low in OL, IL, and KL due to the removal and modification to the aliphatic structure during the extraction process. Pyrolysis mechanism of the synthesized  $\beta$ -O-4 dimer lignin model at a wide temperature range was carried out by Chen et al. [18]. Guaiacol and 4-methoxystyrene were produced from the cleavage of  $\beta$ -O homolysis at a low pyrolysis temperature (300 °C) while both hemolysis and concerted cleavage took place at a medium pyrolysis temperature (500 °C) leading to the formation of carbonyl-containing phenolics. In a high temperature (800 °C), more complex species were produced from the primary pyrolysis products.

In this work, the production of phenol-derived chemicals from organosolv lignin was studied using the Py-GCMS technique. Bagasse was selected as a representative of renewable feedstock for making a comparison with the commercial lignin on pyrolyzed product selectivity. Transformation of lignin structure to monolignol, phenol, and derivatives by pyrolysis was assumed as representative of biochemical production from agricultural wastes. The effect of pyrolysis temperature (400, 500, 600, and 700 °C) on the selectivity of phenolic compounds, such as oxygenated-alkyl methoxy phenol, alkyl methoxy phenol, methoxy phenol, alkyl phenol, and phenol, were thoroughly examined and discussed. The experimental data of the lignin feedstock related to pyrolysis temperature on product selectivity could be applied as a conceptual guideline for further studies on the chemical upgrading process to high-valued biochemical platform and building block.

## 2. Experimental

### 2.1. Biomass

Sugarcane bagasse (BG) was used as starting raw material for lignin extraction using the organosolv method. Firstly, dried BG was pulverized with a blade grinder, and then sieved through 125–425  $\mu$ m stainless steel mesh for further lignin extraction. The commercial grade organosolv lignin (Comm-OS lignin) was procured from the chemical point UG (CP 8068-03-9). Analytical grade ethanol (EtOH) (95%, RCI Labcan) and distilled water (H<sub>2</sub>O) were used as solvents for extracting lignin from BG.

## 2.2. Organosolv lignin extraction process

The extraction of lignin from BG was carried out under autogenous conditions with EtOH and H<sub>2</sub>O in the ratio 75:25 as the extracting agent with a liquid to solid ratio of 1:10. For each trial, 10 g of BG was physically mixed and soaked with the extracting agent for 15 min to ensure adequate homogeneous dispersion through a matrix. The mixing precursor was poured into a 50 ml PTFE-line stainless steel autoclave and subsequently placed in a hot air oven at a temperature of 180 °C for 3 h. Lignin-containing solution was filtered using a filter paper with 5–13 µm pore diameter in order to eliminate BG residue. Subsequently, it was isolated from the filtrate with the help of a rotary evaporator, resulting in precipitation of a dark brown solid called BG lignin, which was dried at 60 °C.

The chemical and elemental composition of lignin were characterized by a proximate analysis with a thermogravimetric analyzer (METTLER TOLEDO; TGA2). The identification of the functional group was performed using Fourier-transform infrared spectroscopy (Perkin Elmer; Spectrum Spotlight 300; FTIR) and the chemical structure was analyzed with nuclear magnetic resonance spectroscopy (BRUKER; AV500; NMR).

## 2.3. Study on phenol production using Py-GCMS technique

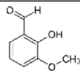
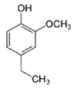
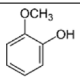
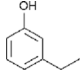
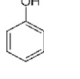
The effect of the conditions of fast pyrolysis on phenol-derived chemical production was studied using Py-GCMS system with experimental setup, as illustrated in Fig. 1. The experiment was conducted using pyrolyzer (Frontier; Py-2020id) with an auto-shot sampler (Frontier; AS1020E) that interfaced with the gas chromatography unit (Thermo Scientific; TRACE 1300) and mass spectrophotometer detector (Thermo Scientific; ISQLT). For each run, 0.4 mg of lignin was placed on a stainless steel crucible and covered with glass wool so as to prevent sample loss during the tests. The sample was dropped into a quartz tube reactor at a set temperature (400, 500, 600, and 700 °C) with helium at 5 ml/min (99.999%) as the carrier gas. The pyrolysis vapors were collected for 30 s prior to injection into the GC unit with a split ratio of 1:100. A low-polarity capillary column (TG-1701MS; 30 m x 0.25 mm; 0.25 mm film thickness; Thermo Scientific) was used for separating the pyrolysis products at a temperature profile of holding at 50 °C for 1 min, further heating it to 280 °C at 4 °C/min and this temperature was held for 10 min. The separated gas was passed through a mass spectrophotometer (MS) detector unit in order to identify chemical compound at a mass-to-charge ratio (m/z) of 20–800 at a 70 eV ionization energy and a 625 amu/s scan speed. Each identified peak was compared with the ones in the National Institute of Standards and Technology (NIST) and Wiley mass spectrum libraries. The distribution of each identified compound was determined with regards to the total peak area according to Eq. (1) [19]. The chemical composition of pyrolyzed vapors were categorized as hydroxyphenyl (H-unit), guaiacyl (G-unit), syringyl (S-unit), aromatic Furan (Aro-Fur), aliphatic hydrocarbon (Ali-HC), aromatic hydrocarbon (Aro-HC), and oxygenated compound (O-comp) with respect to the criteria presented in Table 1. For phenol (H-unit) type, the chemical structure was categorized as oxygenated-alkyl methoxy phenol (OR-Ph-OCH<sub>3</sub>), alkyl methoxy phenol (R-Ph-OCH<sub>3</sub>), methoxy phenol (Ph-OCH<sub>3</sub>), alkyl phenol (R-Ph), and phenol (Ph) with the criteria as shown in Table 2.

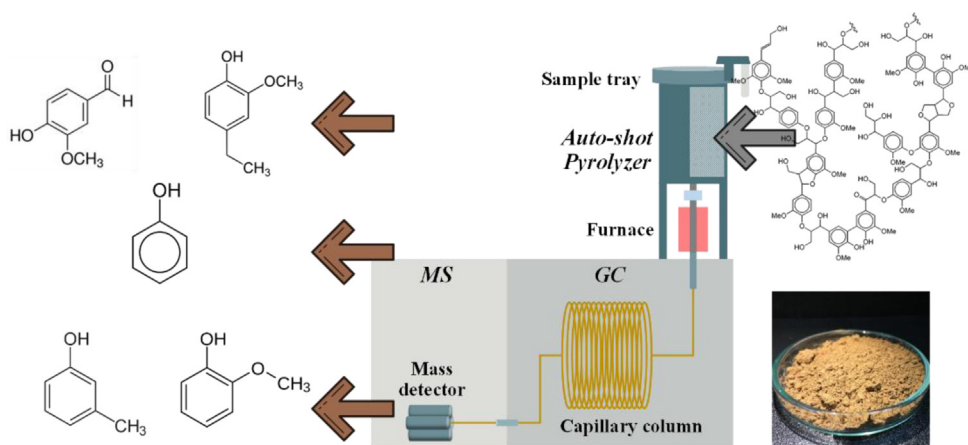
$$\%Compound = \frac{\text{Peak area of target compound}}{\text{Total peak area}} \times 100 \quad (1)$$

**Table 1.** Criteria for pyrolyzed products selectivity.

Categories	Compound	Number of Structure/Functional group			Example
		Aromatic	Aromatic-OH	Aromatic-OCH <sub>3</sub>	
Hydroxyphenyl (H-unit)	Products with hydroxyphenyl unit	1	1	0	Phenol, 3-methyl-
Guaiacyl (G-unit)	Products with guaiacyl unit	1	1	1	Guaiacol, Vanillin
Syringyl (S-unit)	Products with syringyl unit	1	1	2	Syringol
Aliphatic (Ali-HC)	Hydrocarbon with aliphatic structure	0	0	0	Butane
Aromatic (Aro-HC)	Hydrocarbon with aromatic structure	≥1	0	0	Benzene, Toluene
O-compound (O-comp)	O-containing compound	0	0	0	Ester, Carboxylic acid

**Table 2.** Criteria for phenol products identification.

Categories	Compound	Example
Oxygenated-alkyl methoxy phenol (OR-Ph-OCH <sub>3</sub> )	Phenol compound with oxygen containing group along with methoxy group	Vanillin and Phenol, 4-(3-hydroxy-1-propenyl)-2-methoxy- 
Alkyl methoxy phenol (R-Ph-OCH <sub>3</sub> )	Phenol compound with alkyl group along with methoxy group	Phenol, 4-ethyl-2-methoxy- and Phenol, 2-methoxy-3-(2-propenyl)- 
Methoxy phenol (Ph-OCH <sub>3</sub> )	Phenol compound with methoxy group	Phenol, 2-methoxy- and Phenol, 2,6-dimethoxy- 
Alkyl phenol (R-Ph)	Phenol compound with alkyl group	Phenol, 3-methyl- and Phenol, 3,4-dimethyl- 
Phenol (Ph)	Phenol without alkyl and methoxy group	Phenol 

**Fig. 1.** Py-GCMS system.

### 3. Results and discussion

#### 3.1. Lignin characteristics

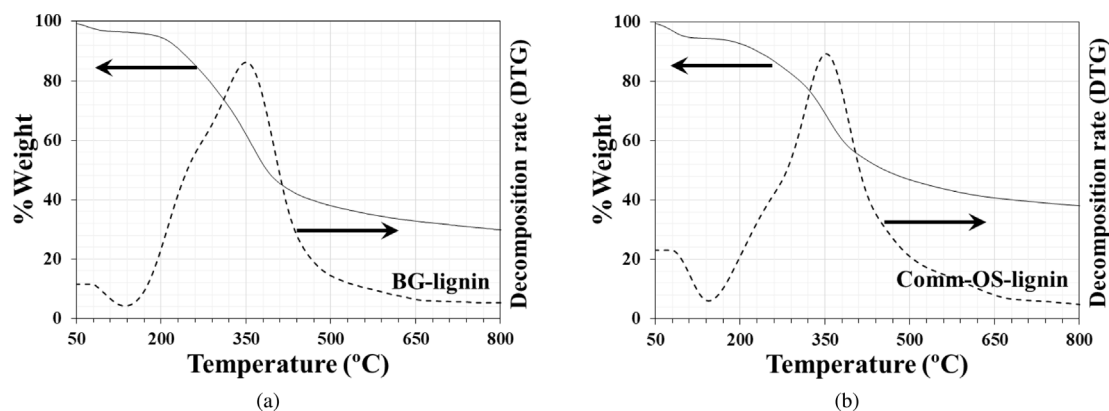
The data from proximate analysis of raw lignin along with other selected samples were presented in [Table 3](#) for comparison. Volatile organic compounds (VOCs) and fixed carbon are the main constituents in both Comm-OS-lignin and BG-lignin that are present at 93.26% and 96.14%, respectively. BG-lignin constituted of higher VOCs while fixed carbon was found in lower quantity than Comm-OS-lignin. Park et al. [20] reported the chemical constituent of isolated lignin from *Miscanthus sacchariflorus* by organosolv process having 55.1% of VOCs and 41.8% of fixed carbon. On the other hand, in soda lignin from sugarcane bagasse, as reported by Naron et al. [21], both VOCs and fixed carbon contents are similar to that obtained in this work. However, ash content of soda lignin (4.50%) was clearly higher than in organosolv process (1.05–0.80%). At 0.09%, ash content in BG-lignin is the

**Table 3.** Chemical composition of raw lignin.

Composition	%Weight			
	Comm-OS-lignin (This work)	BG-lignin (This work)	Organosolv Miscanthus sacchariflorus [20]	Soda bagasse lignin, dry basis [21]
Moisture	5.69	3.78	2.30	–
Volatile matter	56.91	67.34	55.10	66.70
Fixed carbon	36.35	28.80	41.80	29.60
Ash	1.05	0.09	0.80	4.50

lowest, while the combustible portion is higher than 90%, suggesting that it is suitable for biochemical and bio-based material generation with low inorganic impurity, especially for being used as a carbon fiber precursor.

The thermal decomposition profiles under inert atmosphere,  $N_2$ , of Comm-OS-lignin and BG-lignin are displayed in Fig. 2. Both the organosolv lignin displayed a wide degradation region at 150–800 °C with maximum decomposition occurring at a temperature of 350 °C, regarding on the highest decomposition rate as identified by DTG. Extremely high degradation range of lignin might be explained by its high aromatic content in the chemical structure along with numerous branches, side groups, and other chemical bondings [22]. The first decomposition region was found at 50–150 °C, corresponding to evaporation of moisture, while weight loss at 150–800 °C with maximum degradation occurring at 350 °C could be attributed to depolymerization of lignin polymer to oligomer and smaller chemical compound. Huang et al. [16] found two major degradation regions of corncob lignin at 237 °C and 340 °C with final char content of about 30%. Char is a pyrolysis residue of Comm-OS-lignin and BG-lignin, found approximately at 37% and 29%, respectively. From the degradation behavior observed from the TGA trials, pyrolysis temperature of lignin could be targeted at a temperature higher than 400 °C such that degradation trend would approach a plateau region.

**Fig. 2.** Thermal decomposition of (a) Comm-OS-lignin and (b) BG-lignin under inert ( $N_2$ ) atmosphere.

The FTIR spectra of Comm-OS-lignin and BG-lignin are displayed in Fig. 3 along with associated band assignment in Table 4. The vibrations approximately at 1597, 1513, and 1424  $cm^{-1}$  corresponds to C–C stretching of the aromatic skeleton. Broad peak at 3410  $cm^{-1}$  is assigned to the trenching of aliphatic and phenolic hydroxyl (–OH), while vibrations at 2920  $cm^{-1}$  and 2851  $cm^{-1}$  are related to C–H stretching of the aliphatic structure. Aliphatic C–H stretching of BG-lignin shows a higher intensity than that observed in Comm-OS-lignin which is possibly owing to a more aliphatic structure of the former. Vibration at 1694  $cm^{-1}$  can be attributed to the stretching of non-conjugated carbonyl group. The notable signal of G-unit monolignol that presents at 1269  $cm^{-1}$  is for C–O stretching, while 1126  $cm^{-1}$  is assigned to aromatic C–H stretching. In S-unit, designated signals at 1327  $cm^{-1}$  and 834  $cm^{-1}$  are responses from C–O stretching and out-of-plane deformation of aromatic C–H, respectively. The presence of phenolic hydroxyl group resulted from acid hydrolysis of lignin during organosolv process may be noticed at 1371 and 1220  $cm^{-1}$ . Tejado et al. [23] reported that delignification method played an important role in the structure of lignin. For kraft and organosolv processes, the cleavage of  $\beta$ -O-4 and  $\alpha$ -O-4 linkage leaves



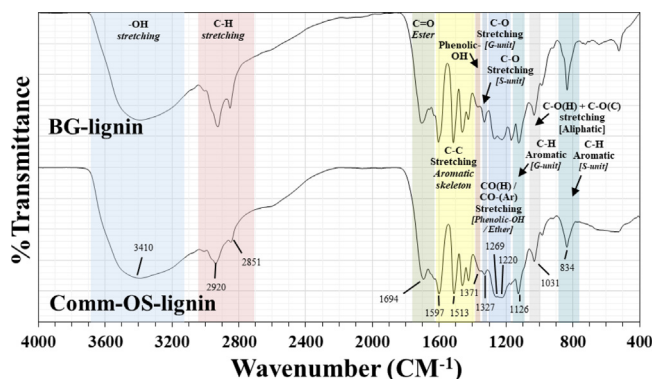


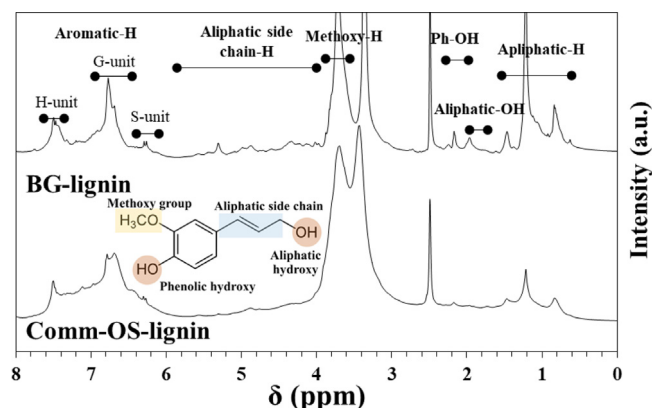
Fig. 3. FTIR spectra of (a) Comm-OS-lignin and (b) BG-lignin.

Table 4. Assignment of FTIR vibration band.

Band (cm <sup>-1</sup> )	Vibration	Assignment
3410	-OH stretching	Phenolic-OH and Aliphatic-OH
2920–2851	C-H stretching	Aliphatic structure, CH <sub>3</sub> , CH <sub>2</sub>
1694	C=O stretching	Non-conjugated carbonyl
1597	C-C stretching	Aromatic skeleton
1513	C-C stretching	Aromatic skeleton
1424	C-C stretching	Aromatic skeleton
1371	O-H in-plane deformation	Phenolic OH
1269	C-O stretching	G-unit
1220	C-O(H) and C-O(Ar) stretching	Phenolic ether and ether
1126	Aromatic C-H in-plane deformation	G-unit
834	Aromatic C-H out-of-plane	S-unit

non-etherified phenolic hydroxy that appears at 1365 cm<sup>-1</sup> vibration signal. In contrast to the soda process, cleavage of aryl-ether bonding is produced, resulting in a low quantity of phenolic hydroxy [24]. G-unit is suspected of being starting reactant for phenol-formaldehyde synthesis due to its free C5 (ortho) position that potentially reacts with formaldehyde through electrophilic substitution reaction, while S-unit exhibits lower activity from linkages at C3 and C5 with the methoxy groups [23].

<sup>1</sup>H-NMR is an essential technique (Fig. 4) for investigation of the features and signal assessment of isolated lignin structure as shown in Table 5. Chemical shift at 8.0–6.1 ppm is attributed to the aromatic proton of monolignol compound, including H-unit, G-unit, and S-unit, while assignment of aliphatic proton is at 1.6–0.4 ppm. Chemical shift signal of aliphatic structure of BG-lignin is quite higher and sharper than Comm-OS-lignin, possibly since the isolation process facilitates to less C–C bond cleavage and results in higher aliphatic content. The stronger chemical shift of proton in aliphatic side chain at 6.0–4.0 ppm found in BG-lignin proves that it has a higher aliphatic structure than Comm-OS-lignin. The signal at 7.7–7.3 ppm is assigned to aromatic proton in H-unit, 7.1–6.5 ppm could be attributed to G-unit, and 6.4–6.1 ppm is assigned to S-unit [25–27]. The peak area and intensity of aromatic proton is strongly related to their molecular weight and amount of phenolic hydroxyl in each monolignol unit. The strength of the peak at 4.0–3.5 ppm is attributed to the proton in methoxy group; 3.4–3.1 ppm is assigned to proton in water and 2.50 ppm to the chemical shift of proton in a solvent (DMSO; Dimethyl sulfoxide). Phenolic hydroxyl group and aliphatic hydroxyl group are attributed at 2.3–2.1 ppm and 2.1–1.8 ppm, respectively. In Table 6, the H/G/S fraction and phenolic hydroxyl to aliphatic hydroxy ratio (OH<sub>Ph</sub>/OH<sub>Al</sub>) that are calculated from integral of each represented signal are presented. G-unit monolignol in BG-lignin (0.82) is slightly higher than that in Comm-OS-lignin (0.71), which corresponds to biomass feedstock and the isolation process parameters. In addition, difference in phenolic hydroxy and aliphatic hydroxy content in both lignin were observed. Most of the hydroxy content in Comm-OS-lignin bonded with aromatic ring and responded with a high OH<sub>Ph</sub>/OH<sub>Al</sub> ratio of 4.33. In contrast with BG-lignin, hydroxy content was almost even in phenolic hydroxy and aliphatic hydroxy at 0.44 and 0.56, respectively. From these results, it can be concluded that BG-lignin contain greater aliphatic hydrocarbon

Fig. 4.  $^1\text{H}$ -NMR of raw lignin.Table 5.  $^1\text{H}$ -NMR assignment of selected chemical components.

Signal (ppm)	Assignment
7.7–7.30	Aromatic-H in H-unit
7.1–6.5	Aromatic-H in G-unit
6.4–6.1	Aromatic-H in S-unit
6.0–4.0	Aliphatic side chain H
4.0–3.5	Methoxy-H
3.4–3.1	Water-H
2.5	DMSO (solvent)
2.3–2.1	Phenolic hydroxyl
2.1–1.8	Aliphatic hydroxyl
1.6–0.4	Aliphatic-H

Table 6. Chemical of lignin studied by  $^1\text{H}$ -NMR.

Lignin	Monolignol fraction			Hydroxy group fraction		$\text{OH}_{\text{Ph}}/\text{OH}_{\text{Ali}}$
	H-unit	G-unit	S-unit	Phenolic-OH	Aliphatic-OH	
Comm-OS-lignin	0.26	0.71	0.03	0.81	0.19	4.33
BG-lignin	0.16	0.82	0.02	0.44	0.56	0.79

structure in propyl group as well as others than that of Comm-OS-lignin. As a consequence, the selectivity of pyrolytic products of two lignin feedstock may possibly be distinct due to deviation of hydroxy group and aliphatic structure content.

### 3.2. Fast pyrolysis of lignin using Py-GCMS

Py-GCMS technique was employed to rapidly pyrolyze lignin and in the real-time analysis of devolatilized products. Chromatograms of these products from Comm-OS-lignin and BG-lignin as identified by the GCMS technique are illustrated in Fig. 5. From the results, it was found that there is a slight difference in the detection of chemical species between Comm-OS-lignin and BG-lignin. In Comm-OS-lignin, signal of carbon dioxide ( $\text{CO}_2$ ) was detected at a retention time (RT) of 3.02 min, while methanol ( $\text{CH}_3\text{OH}$ ) was found at 3.34 min. This finding was also reported in Brebu et al. [28], a study of pyrolysis of organosolv and kraft lignin. Liu et al. and Kawamoto et al. [29,30] suggested the pyrolysis pathway of G-type lignin model compound containing  $\beta$ -O-4 ether linkage. Cleavage of lignin dimer unit is strongly related to the bonding energy among  $\text{C}_\alpha$ - $\text{C}_\beta$ ,  $\text{C}_\beta$ -O, and O-4. Cleavage of lower bonding energy linkage as that of  $\text{C}_\alpha$ - $\text{C}_\beta$  (103.8 kcal/mol) and  $\text{C}_\beta$ -O (90.9 kcal/mol) and the continuous elimination of methoxy ( $-\text{O}-\text{CH}_3$ ), aromatic substitution group, with methanol as a byproduct, are due to the fact that O-4 is most stable with a bonding energy of 137.2 kcal/mol. The peak intensity of  $\text{CO}_2$  is significantly



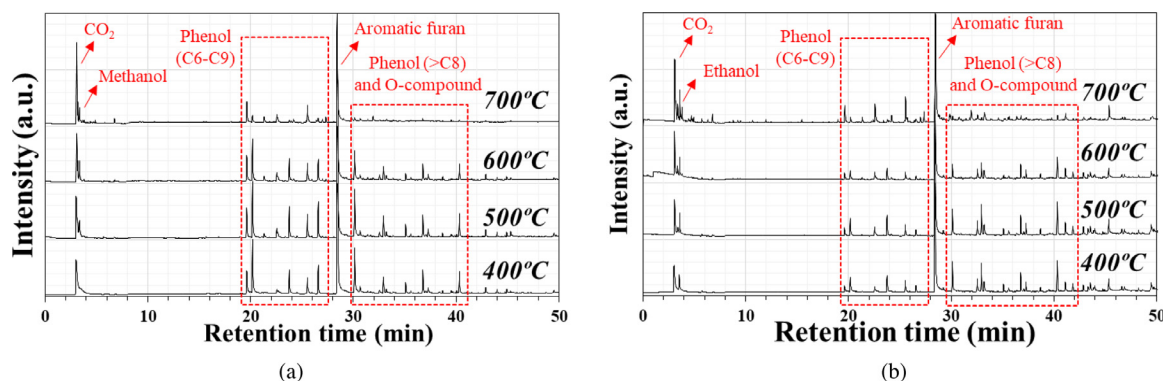


Fig. 5. Chromatogram of pyrolyzed products from (a) Comm-OS-lignin and (b) BG-lignin.

increased with the pyrolysis temperature which is responsible for the breakdown of byproducts of high molecular weight lignin to smaller phenols building units such as p-hydroxyphenyl unit (H-unit), guaiacyl unit (G-unit), and syringyl unit (S-unit) [31]. During RT 19–28 min, a phenol compound was detected that was mostly of C6–C9 carbon members, while those larger than C8 were found at RT 30–42 min. High quantity of aromatic furan (34.24–50.39%), such as 2,3-dihydrobenzofuran, detected at RT 28.44 min could be measured for all pyrolysis temperature. Chromatograms of BG-lignin also revealed similar chemical species trend in which phenol and derivatives were the main compounds. However, 30.75–38.83% of 2,3-dihydrobenzofuran was also detected, which was slightly lower than those from Comm-OS-lignin. Ryu et al. [32] reported 12.12% benzofuran from pyrolysis of commercial kraft lignin, while according to Liu et al. [29], 24.1% 2,3-dihydrobenzofuran was also noted as a major contributor of pyrolysis products from H-type lignin model compound with only 3.37% from G-type at a reaction temperature of 600 °C.

Selectivity of the chemical compounds obtained from fast pyrolysis of Comm-OS-lignin and BG-lignin was illustrated in Fig. 6 and Fig. 7, respectively. As mentioned before, the highest identifiable chemical species were aromatic furan (2,3-dihydrobenzofuran), in which their quantity increased with the pyrolysis temperature from 400–700 °C. Lin et al. [33] reported that furan compound (18.4% 2,3-dihydrobenzofuran) at 26.3% is the most abundant product generated from the pyrolysis of wheat straw sulfonate lignin, while the lignin materials isolated from enzymatic and alkali process had less than 7% of similar products. Moreover, they concluded that lignin isolation process significantly affected the selectivity of speciation of pyrolyzed products. The production pathway of 2,3-dihydrobenzofuran from lignin degradation was unclear as a result of several concurrent reactions such as cleavage of ether bond between lignin monomer simultaneously with structure rearrangement. Lou et al. [34] studied the pyrolysis of enzymatic/mild acidolysis lignin isolated from moso bamboo (grass biomass). Heterocyclic 2,3-dihydrobenzofuran was dominant at a low temperature (250–400 °C), giving the highest yield of 66.26% at 320 °C. The conversion of 2,3-dihydrobenzofuran to phenol (20%) occurred by increasing the pyrolysis temperature to 800 °C. Thus, they presented a possible pathway of 2,3-dihydrobenzofuran production from lignin pyrolysis that resulted from the occurrence of a radically induced reaction of o-quinone methide. Quinone methide is chiefly an intermediate product of C $\alpha$ -O cleavage during the primary pyrolysis stage that subsequently rearranged to cyclic structure by H-abstraction of allyl radical to 2,3-dihydrobenzofuran [35].

H-unit, G-unit, and S-unit pyrolyzates are distributed at a pyrolysis temperature of 400–600 °C according to the same fraction with H/G/S ratio of 1/1/0.7 and 0.8/1/1 for Comm-OS-lignin and BG-lignin, respectively (Fig. 8). The above ratio corresponds well with the herbaceous biomass that has a similar distribution of H-unit, G-unit, and S-unit monolignol. The ratio of S-unit and G-unit (S/G) is considered as a value to help determine the recalcitrance of biomass to bioconversion. In this work, S/G of BG-lignin (1.0–1.06) is higher than that of Comm-OS-lignin (0.61–0.71). Dumitrache et al. [36] suggested that high S/G ratio is related to linear chain and higher molecular weight of lignin. Unfortunately, the correlation of S/G ratio on biomass conversion is not uniform across the various feedstock [37]. Increasing the temperature to 700 °C displayed a significant selectivity enhancement on H-unit with the highest content of 28.82% for Comm-OS-lignin and 29.66% for BG-lignin. S-unit was derived only from syringol alcohol monomer and could be fragmented into G-unit and H-unit through

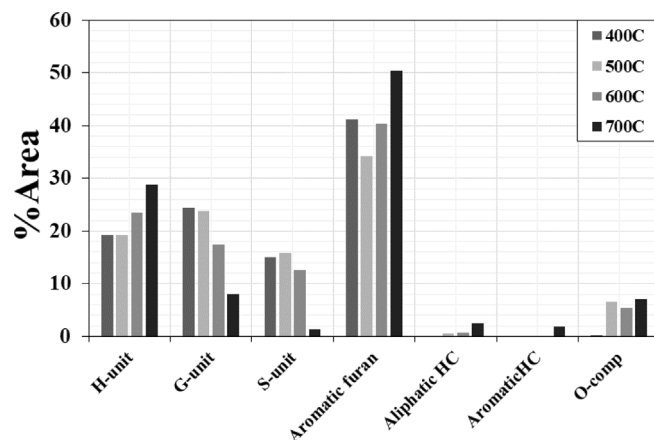


Fig. 6. Chemical selectivity of the pyrolyzed products from Comm-OS-lignin.

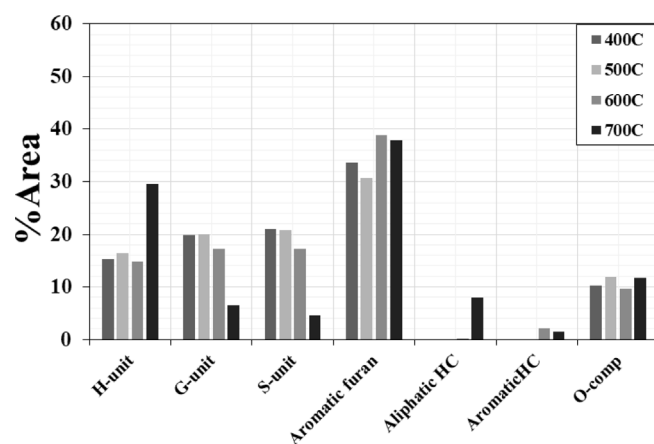


Fig. 7. Chemical selectivity of the pyrolyzed products from BG-lignin.

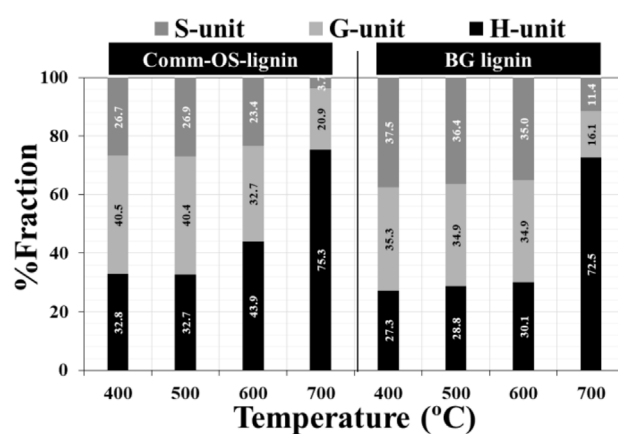


Fig. 8. Distribution of H-unit, G-unit, and S-unit of the pyrolyzed products.

a demethoxylation reaction [38,39]. Compared with the lignin isolation from the kraft process with eucalyptus wood [40], the distribution of monolignol of the pyrolyzed products obtained from 400–600 °C was mainly G-unit

and S-unit, while H-unit with minor content was detected at 600 °C. This indicates that the isolation process and the biomass feedstock significantly affect monolignol species.

The reduction of H-unit and S-unit lignin with a simultaneous increase of H-unit and aromatic hydrocarbon was observed for both Comm-OS-lignin and BG-lignin, which corresponded with Shen et al. [41], who studied the pyrolysis of alkali lignin from different feedstock. The demethoxylation reaction of the methoxy group of G-unit and S-unit was carried out at a high temperature, resulting in remarkably enhanced H-unit and slightly aromatic HC products. Liu et al. [42] studied phenol production from alkali lignin in contrast to organosolv lignin. The selectivity of phenol, carbonyl, and hydrocarbon was considerably different between lignin isolation processes. The selectivity of phenol from the organosolv lignin was always higher at 400–600 °C due to greater  $\beta$ -O-4 linkage contents. BG-lignin yielded more hydrocarbon products than Comm-OS-lignin (9.47% and 4.31% at 700 °C respectively). Thus, the dehydroxylation and dealkylation reactions of the monolignol compound produced from BG-lignin was shown to be slightly more vigorous than that obtained from Comm-OS-lignin. Oxygenated compounds were detected from 0.20–7.05% and 9.57–11.74% for Comm-OS-lignin and BG-lignin, respectively, which were byproducts of the dealkylation of the alkyl group.

Phenol and its derivatives are attractive bio-resource feedstock with the potential to be used as important precursors for biochemical industry, pharmaceutical industry, and others. The phenolic compound production from fast pyrolysis of Comm-OS-lignin and BG-lignin is shown in Table 7 and Table 8, respectively. For the Comm-OS-lignin pyrolysis, phenol, 2-methoxy- (9.83%, 500 °C), phenol, 2,6-dimethoxy- (8.31%, 500 °C), phenol, 4-ethyl-2-methoxy- (4.87%, 600 °C), and cresol (4.59%, 500 °C) were observed in higher proportions than other phenolic compounds at 400–600 °C. For the BG-lignin, phenol, 2,6-dimethoxy- (5.24%, 500 °C) and phenol, 2,6-dimethoxy-4-(2-propenyl)- (5.35%, 500 °C), phenol, 4-methoxy-3-(methoxymethyl)- (4.85%, 500 °C), phenol, 3-(1,1-dimethylethyl)-4-methoxy- (3.17%, 500 °C), and vanillin (2.35%, 500 °C) were found in a higher proportion. These monolignols were detected as the dominant products from the hydrothermal carbonization of bagasse lignin, as reported by Du et al. [43]. Cresol (o-cresol and m-cresol) was produced from lignin with a proportion of 1.64–5.95% and 1.29–6.15% from Comm-OS-lignin and BG-lignin, respectively and was enhanced by the pyrolysis temperature. Vanillin was also found at 2.33–2.41% with BG-lignin as the raw material. It is an important chemical feedstock, as it constitutes the aromatic building block for various chemical industries. Nowadays, vanillin is being produced at an industrial scale of 20,000 ton/year [44]. Of this, 15% comes from lignin [45]. In general, vanillin is synthesized from petroleum-based intermediate, especially guaiacol or phenol, 2-methoxy- [46] under catalytic conditions. Most of the phenol compounds detected in the pyrolysis products from both feedstock present aromatic skeletons with various aromatic substituted side groups.

Guaiacol and syringol are the most common products generated from the primary pyrolysis of lignin at a temperature of 200–400 °C that subsequently transformed to catechol, pyrogallol, and cresol along with phenol by C–C cracking of side chain during secondary pyrolysis at 400–450 °C. This results in the increase in the monomer content [35]. Generation of guaiacol and syringol could be explained by two possible radical chain pathways; first is the hydrogen abstraction of C $\alpha$ -H of lignin oligomer and the second is the hydrogen abstraction of phenolic hydroxyl group. The final products of both these reactions are guaiacol and syringol. However, the hydrogen abstraction of phenolic hydroxyl group seemed to be more effective when the temperature is set at 260 °C [35]. The hydrogen abstraction of phenolic hydroxyl group was enhanced by means of intermediated radicals under pyrolysis environment [47], resulting in a cleavage of  $\beta$ -ether bonds to form a quinone methide intermediate and is further cleaved to guaiacol and syringol. Furthermore, quinone methide intermediates also cleave and rearrange themselves in a cyclical structure as 2,3-dihydrobenzofuran.

In order to investigate the thermal effect on phenolic selectivity which occurred during the secondary pyrolysis, the chemical structure of the phenolic compound was categorized as oxygenated-alkyl methoxy phenol (OR–Ph–OCH<sub>3</sub>), alkyl methoxy phenol (R–Ph–OCH<sub>3</sub>), methoxy phenol (Ph–OCH<sub>3</sub>), alkyl phenol (R–Ph), and phenol (Ph). The selectivity of the phenolic compound originating from the Comm-OS-lignin and BG-lignin pyrolysis at various temperatures are displayed in Fig. 9 and Fig. 10, respectively. Temperature is a key player of phenolic selectivity, as it enhances the cleavage of methoxy and others aromatic substitution groups [48]. The cleavage of strong aromatic and aliphatic side chain bonding are driven by the hydrogen transfer reaction in aromatic ring during the secondary pyrolysis [49,50]. Thus, transformation of primary pyrolysis products, including guaiacol and syringol to phenol compound, could possibly proceed in the following order. First, the elimination of oxygen atom from oxygenated-alkyl methoxy phenol (OR–Ph–OCH<sub>3</sub>) at C4 position due to deoxygenation

**Table 7.** Phenol products from Comm-OS-lignin pyrolysis at various temperature.

RT (min)	Formula	Compound	%Area			
			400 °C	500 °C	600 °C	700 °C
19.62	C <sub>6</sub> H <sub>6</sub> O	Phenol	5.47	5.34	5.28	7.89
20.20	C <sub>7</sub> H <sub>8</sub> O <sub>2</sub>	Phenol, 2-methoxy-	11.69	9.83	8.08	2.35
21.31	C <sub>7</sub> H <sub>8</sub> O	Phenol, 2-methyl- (o-Cresol)	–	0.66	0.86	1.77
22.21	C <sub>8</sub> H <sub>8</sub> O <sub>2</sub>	3-Hydroxy-4-methylbenzaldehyde	–	–	–	0.10
22.57	C <sub>7</sub> H <sub>8</sub> O	Phenol, 3-methyl- (m-Cresol)	1.64	2.37	2.51	4.18
23.76	C <sub>8</sub> H <sub>10</sub> O <sub>2</sub>	Creosol	4.05	4.59	4.05	0.74
23.97	C <sub>8</sub> H <sub>10</sub> O	Phenol, 3-ethyl-	–	–	–	0.37
24.15	C <sub>8</sub> H <sub>10</sub> O	Phenol, 3,4-dimethyl-	–	0.23	0.44	1.22
25.53	C <sub>8</sub> H <sub>10</sub> O	Phenol, 4-ethyl-	3.07	3.62	3.48	6.91
26.39	C <sub>10</sub> H <sub>14</sub> O <sub>2</sub>	(6-Hydroxymethyl-2,3-dimethylphenyl)methanol	–	–	–	0.60
26.58	C <sub>9</sub> H <sub>12</sub> O <sub>2</sub>	Phenol, 4-ethyl-2-methoxy-	4.46	4.87	–	1.51
26.98	C <sub>9</sub> H <sub>12</sub> O	Phenol, 4-ethyl-3-methyl-	–	–	–	0.94
27.33	C <sub>9</sub> H <sub>12</sub> O	Phenol, 3-(1-methylethyl)-	–	–	–	1.46
29.04	C <sub>10</sub> H <sub>14</sub> O	2,5-Diethylphenol	0.66	–	–	0.58
29.23	C <sub>11</sub> H <sub>16</sub> O	2-Ethyl-5-n-propylphenol	–	–	–	–
29.32	C <sub>10</sub> H <sub>12</sub> O <sub>3</sub>	Phenol, 4-(3-hydroxy-1-propenyl)-2-methoxy-	–	0.48	–	–
29.82	C <sub>9</sub> H <sub>10</sub> O	2-Allylphenol	–	–	0.22	1.79
30.13	C <sub>8</sub> H <sub>10</sub> O <sub>3</sub>	Phenol, 2,6-dimethoxy-	8.79	8.31	6.44	1.09
30.65	C <sub>9</sub> H <sub>10</sub> O	2-Allylphenol	1.50	–	–	1.13
31.41	C <sub>9</sub> H <sub>10</sub> O <sub>4</sub>	Benzoic acid, 2-hydroxy-4-methoxy-6-methyl-	0.21	0.29	0.37	0.30
31.91	C <sub>10</sub> H <sub>12</sub> O	Phenol, 2-(2-methyl-2-propenyl)-	–	–	–	1.59
32.56	C <sub>10</sub> H <sub>12</sub> O <sub>2</sub>	Phenol, 2-methoxy-6-(1-propenyl)-	0.47	0.74	0.78	0.20
32.93	C <sub>9</sub> H <sub>12</sub> O <sub>3</sub>	Phenol, 4-methoxy-3-(methoxymethyl)-	2.57	2.85	2.16	–
33.18	C <sub>8</sub> H <sub>8</sub> O <sub>3</sub>	Vanillin	0.69	0.75	–	–
33.87	C <sub>10</sub> H <sub>12</sub> O <sub>3</sub>	Phenol, 4-(3-hydroxy-1-propenyl)-2-methoxy-	–	–	0.22	0.29
35.11	C <sub>10</sub> H <sub>14</sub> O <sub>3</sub>	5-tert-Butylpyrogallol	1.56	1.66	1.04	–
35.59	C <sub>10</sub> H <sub>14</sub> O <sub>2</sub>	Phenol, 3-methoxy-2,4,6-trimethyl-	0.32	0.40	0.40	–
36.76	C <sub>11</sub> H <sub>16</sub> O <sub>2</sub>	Phenol, 3-(1,1-dimethylethyl)-4-methoxy-	3.83	3.23	2.93	0.56
37.07	C <sub>10</sub> H <sub>12</sub> O <sub>3</sub>	Phenol, 4-(3-hydroxy-1-propenyl)-2-methoxy-	0.36	0.48	–	–
37.28	C <sub>11</sub> H <sub>14</sub> O <sub>3</sub>	Phenol, 2,6-dimethoxy-4-(2-propenyl)-	0.93	1.22	0.94	–
38.68	C <sub>11</sub> H <sub>14</sub> O <sub>3</sub>	Phenol, 2,6-dimethoxy-4-(2-propenyl)-	0.33	0.47	0.51	–
39.66	C <sub>12</sub> H <sub>16</sub> O <sub>2</sub>	Phenol, 2-(1-methyl-2-butenyl)-4-methoxy-	–	0.20	–	–
40.06	C <sub>11</sub> H <sub>14</sub> O <sub>4</sub>	Methyl 3-(4-hydroxy-3-methoxyphenyl) propanoate	0.25	0.32	–	–
40.31	C <sub>11</sub> H <sub>14</sub> O <sub>3</sub>	Phenol, 2,6-dimethoxy-4-(2-propenyl)-	3.31	3.18	2.76	0.33
41.10	C <sub>9</sub> H <sub>10</sub> O <sub>4</sub>	Benzaldehyde, 4-hydroxy-3,5-dimethoxy-	0.18	0.32	0.44	–
42.86	C <sub>10</sub> H <sub>12</sub> O <sub>4</sub>	Ethanone, 1-(4-hydroxy-3,5-dimethoxyphenyl)-	0.97	1.09	1.09	–
43.97	C <sub>11</sub> H <sub>14</sub> O <sub>4</sub>	trans-Sinapyl alcohol	0.46	0.51	0.34	–
44.93	C <sub>11</sub> H <sub>12</sub> O <sub>4</sub>	trans-Sinapaldehyde	0.71	0.65	–	–
<b>Total</b>			<b>58.47</b>	<b>58.69</b>	<b>43.35</b>	<b>37.88</b>

reaction, resulting in alkyl phenol methoxy (R–Ph–OCH<sub>3</sub>) and phenol methoxy (Ph–OCH<sub>3</sub>) products. The cleavage of methoxy group continuously takes place in order to form phenol (Ph) and alkyl phenol (R–Ph) products, especially at a high temperature. However, transformation of phenol to gas as a result of phenoxy radical decomposition into permanent gas and smaller molecules was reported [35]. Nevertheless, the details regarding the decomposition mechanism is still not well understood. Partial decomposition of suspected phenol compound is exhibited in Fig. 11, in which the total phenol production considerably decreases from 58.47% (400 °C) to 37.88% (700 °C) and 53.35% (400 °C) to 39.23% (700 °C) for Comm-OS-lignin and BG-lignin, respectively.

The selectivity of particular phenolic compounds from different lignin feedstock is observed. For Comm-OS-lignin, methoxy phenol is a major compound as a result of pyrolysis at 400 °C, 500 °C, and 600 °C with product quantities of 25.99%, 23.24%, and 18.92%, respectively. This result corresponds with Fan et al. [51] that reported methoxy phenol (57.6%) and alkyl methoxy phenol (32.4%) as the major parts of phenolic compounds from co-pyrolysis of alkali lignin and waste cooking oil at 550 °C. Increasing the temperature to 700 °C showed significantly reduction of methoxy phenol contents to 4.18%, while alkyl phenol (R–Ph) was enhanced to 22.52% from 8.56%.

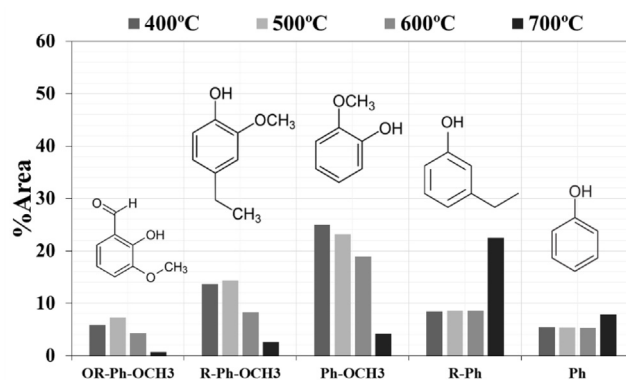


Fig. 9. Phenolic selectivity of pyrolyzed products of Comm-OS-lignin.

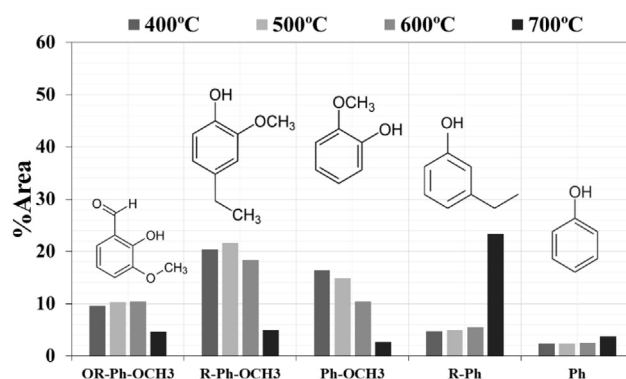


Fig. 10. Phenolic selectivity of pyrolyzed products of BG-lignin.

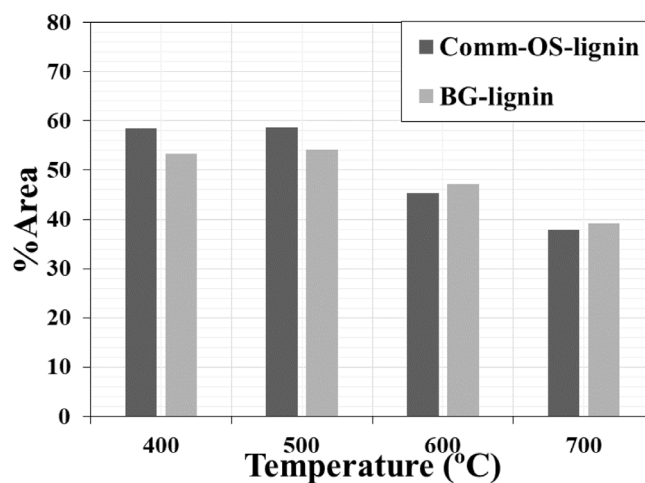


Fig. 11. Total phenol production from lignin.

The selectivity of oxygenated-alkyl methoxy phenol (OR-Ph-OCH<sub>3</sub>) and alkyl methoxy phenol (R-Ph-OCH<sub>3</sub>) is related to the pyrolysis temperature in the same fashion, as methoxy phenol is reduced dramatically when

**Table 8.** Phenol products from BG-lignin pyrolysis at various temperature.

RT (min)	Formula	Compound	%Area			
			400 °C	500 °C	600 °C	700 °C
19.62	C <sub>6</sub> H <sub>6</sub> O	Phenol	1.39	1.42	1.70	3.70
20.16	C <sub>7</sub> H <sub>8</sub> O <sub>2</sub>	Phenol, 2-methoxy-	3.46	3.09	2.16	0.91
21.31	C <sub>7</sub> H <sub>8</sub> O	Phenol, 2-methyl- (o-cresol)	–	–	0.24	1.01
22.54	C <sub>7</sub> H <sub>8</sub> O	Phenol, 3-methyl- (m-cresol)	1.29	1.96	2.10	5.14
23.76	C <sub>8</sub> H <sub>10</sub> O <sub>2</sub>	Creosol	3.15	3.32	2.30	0.47
24.15	C <sub>8</sub> H <sub>10</sub> O	Phenol, 3,4-dimethyl-	–	–	0.34	1.59
25.51	C <sub>8</sub> H <sub>10</sub> O	Phenol, 4-ethyl-	2.27	1.99	1.91	6.46
26.56	C <sub>9</sub> H <sub>12</sub> O <sub>2</sub>	Phenol, 4-ethyl-2-methoxy-	1.01	0.94	0.57	0.74
26.98	C <sub>9</sub> H <sub>12</sub> O	Phenol, 4-ethyl-3-methyl-	–	–	–	0.88
27.33	C <sub>9</sub> H <sub>12</sub> O	Phenol, 3-(1-methylethyl)-	–	–	–	1.66
29.05	C <sub>10</sub> H <sub>14</sub> O	2,5-Diethylphenol	–	–	–	0.81
29.23	C <sub>10</sub> H <sub>12</sub> O <sub>2</sub>	Phenol, 2-methoxy-3-(2-propenyl)-	0.85	0.88	0.88	0.73
29.82	C <sub>9</sub> H <sub>10</sub> O	2-Allylphenol	–	–	–	2.24
30.11	C <sub>8</sub> H <sub>10</sub> O <sub>3</sub>	Phenol, 2,6-dimethoxy-	6.45	5.24	3.71	1.22
30.74	C <sub>9</sub> H <sub>10</sub> O	2-Allylphenol	–	–	–	0.88
30.95	C <sub>10</sub> H <sub>12</sub> O <sub>2</sub>	Phenol, 2-methoxy-4-(1-propenyl)-	–	–	0.30	–
31.93	C <sub>9</sub> H <sub>10</sub> O	Phenol, 4-(2-propenyl)-	–	–	0.40	2.71
32.54	C <sub>10</sub> H <sub>12</sub> O <sub>2</sub>	Phenol, 2-methoxy-6-(1-propenyl)-	2.25	2.42	2.48	1.34
32.93	C <sub>9</sub> H <sub>12</sub> O <sub>3</sub>	Phenol, 4-methoxy-3-(methoxymethyl)-	4.62	4.85	3.19	–
33.18	C <sub>8</sub> H <sub>8</sub> O <sub>3</sub>	Vanillin	2.33	2.35	2.41	2.39
35.09	C <sub>10</sub> H <sub>14</sub> O <sub>3</sub>	5-tert-Butylpyrogallol	1.17	0.96	0.56	–
35.59	C <sub>10</sub> H <sub>14</sub> O <sub>2</sub>	Phenol, 3-methoxy-2,4,6-trimethyl-	0.65	0.66	0.55	–
36.76	C <sub>11</sub> H <sub>16</sub> O <sub>2</sub>	Phenol, 3-(1,1-dimethylethyl)-4-methoxy-	3.18	3.17	3.11	0.75
37.07	C <sub>10</sub> H <sub>12</sub> O <sub>3</sub>	Phenol, 4-(3-hydroxy-1-propenyl)-2-methoxy-	–	–	0.43	–
37.28	C <sub>11</sub> H <sub>14</sub> O <sub>3</sub>	Phenol, 2,6-dimethoxy-4-(2-propenyl)-	1.67	1.82	1.68	0.65
38.68	C <sub>11</sub> H <sub>14</sub> O <sub>3</sub>	Phenol, 2,6-dimethoxy-4-(2-propenyl)-	0.75	1.02	1.08	–
39.66	C <sub>12</sub> H <sub>16</sub> O <sub>2</sub>	Phenol, 2-(1-methyl-2-butenyl)-4-methoxy-	–	0.31	–	–
39.89	C <sub>11</sub> H <sub>12</sub> O <sub>3</sub>	Benzaldehyde, 3-hydroxy-4-methoxy-2-(2-propenyl)-	–	0.28	–	–
40.31	C <sub>11</sub> H <sub>14</sub> O <sub>3</sub>	Phenol, 2,6-dimethoxy-4-(2-propenyl)-	5.32	5.35	4.53	0.71
41.10	C <sub>9</sub> H <sub>10</sub> O <sub>4</sub>	Benzaldehyde, 4-hydroxy-3,5-dimethoxy-	2.07	2.53	2.75	1.57
42.86	C <sub>10</sub> H <sub>12</sub> O <sub>4</sub>	Ethanone, 1-(4-hydroxy-3,5-dimethoxyphenyl)-	1.12	1.34	1.27	–
43.32	C <sub>10</sub> H <sub>12</sub> O <sub>3</sub>	Phenol, 4-(3-hydroxy-1-propenyl)-2-methoxy-	1.02	1.23	1.00	–
43.53	C <sub>12</sub> H <sub>16</sub> O <sub>4</sub>	Ethyl-β-(4-hydroxy-3-methoxy-phenyl)-propionate	2.10	1.98	1.82	0.67
43.97	C <sub>11</sub> H <sub>14</sub> O <sub>4</sub>	trans-Sinapyl alcohol	1.77	1.70	1.25	–
46.60	C <sub>12</sub> H <sub>14</sub> O <sub>4</sub>	Ethyl (2E)-3-(4-hydroxy-3-methoxyphenyl)-2-propenoate	0.95	0.86	0.68	–
46.85	C <sub>11</sub> H <sub>12</sub> O <sub>3</sub>	p-Hydroxycinnamic acid, ethyl ester	0.91	0.94	0.86	–
49.72	C <sub>11</sub> H <sub>14</sub> O <sub>4</sub>	trans-Sinapyl alcohol	1.60	1.52	0.94	–
<b>Total</b>			<b>53.35</b>	<b>54.15</b>	<b>47.22</b>	<b>39.23</b>

temperature raised to 700 °C. Meanwhile, the selectivity to phenol was quite stable at 5.28–7.89% even at an increased temperature. For BG-lignin, alkyl methoxy phenol was found as a dominant structure at 18.38–21.70%, while methoxy phenol was found to be 10.36–16.42% at 400–600 °C. The appearance of alkyl methoxy phenol as the main component of BG-lignin may straightforwardly be explained by its higher aliphatic structure that Comm-OS-lignin as detected by <sup>1</sup>H-NMR. The significant increase of alkyl phenol (23.38%) was also detected, similar to Comm-OS-lignin when the temperature raised to 700 °C. Abundance of alkyl phenol selectivity is strongly related to the cleavage of aromatic side chains, such as oxygen-containing group, alkyl group, and methoxy group.

From the Py-GCMS experiment, it can be noted that most of the phenolic compound selectivity obtained from Comm-OS-lignin and BG-lignin through fast pyrolysis at 400–600 °C result in the formation of methoxy phenol and alkylated phenol, while, even though the temperature is raised to 700 °C, the phenol yield is lower than 8%. This observation concurs Diehl et al. [13], in which the char produced from pyrolysis of softwood and hardwood lignin at 250–600 °C is analyzed using <sup>13</sup>C-NMR techniques. The oxygen functional groups were quickly evolved at 500 °C, leading to an aromatic carbon spinning signal. The low phenol production could possibly be explained by complexity and instability of the radical cleavage of lignin oligomer during pyrolysis. This means that the



repolymerization of intermediate radicals and ions of pyrolysis vapors generally occurs and results in the aromatic substitution side group. Thus, a thermal process is not sufficient to transform lignin to a high-valued chemical such as phenol and derivatives. The highly selective molecular sieve catalysts are extremely essential to enhance the production of valued chemicals, such as vanillin, benzene, toluene, xylene, and other aromatics, that are used as chemical feedstock for chemistry industrial, food, pharmaceutical, and cosmetic industries.

#### 4. Conclusion

The production of phenol-derived chemicals extracted from organosolv lignin was studied using Py-GCMS technique, in which bagasse from the local industry was used as raw materials (BG-lignin) and evaluated with commercial organosolv lignin (Comm-OS-lignin). BG-lignin exhibited a slight difference in term of its chemical and structural composition as compared to Comm-OS-lignin. Combustible constituents, such as volatile organic compounds (VOCs) and fixed carbon of both lignins, are quite similar with about 93.26% and 96.14% of the Comm-OS-lignin and BG-lignin, respectively, while BG-lignin displayed a significantly lower ash of 0.09%. This may be due to the difference in the reaction that occurred during the isolation process and the obtained molecular weight of lignin. The thermal degradation behavior of Comm-OS-lignin and BG-lignin was observed at a wide decomposition range of 150–800 °C, wherein the highest degree of degradation took place at a temperature of about 350 °C. The identification of the functional groups using FT-IR reported significant vibration signal of guaiacyl (G-unit) and syringyl (S-unit), which are monolignol structures with high hydroxyl group content. Although Comm-OS-lignin and BG-lignin were similarly isolated using the organosolv process, significant variation in the aromatic and aliphatic contents was still identified by <sup>1</sup>H-NMR. Due to greater aliphatic hydroxy content, chemical shift signal of aliphatic proton in BG-lignin is stronger than that in Comm-OS-lignin. Benzofuran emerged as a dominant species from fast pyrolysis of lignin using the Py-GCMS instrument, and it was suspected of being a product from C $\alpha$ -O cleavage during the primary pyrolysis stage. Demethoxylation reaction of methoxy group of G-unit and S-unit is dominated at a high temperature that results in a vastly enhanced H-unit and slightly on aromatic hydrocarbon products. BG-lignin reaction showed the abundant hydrocarbon production, with 9.47% at 700 °C from dealkylation of monolignol compound, was more vigorous than that in Comm-OS-lignin. Phenolic selectivity of pyrolyzed products from Comm-OS-lignin and BG-lignin at 400–600 °C mainly include methoxy phenol (Ph-OCH<sub>3</sub>) and alkylated methoxy phenol (R-Ph-OCH<sub>3</sub>), respectively. A higher pyrolysis temperature of 700 °C led to the elimination of aromatic side group and promoted alkyl phenol selectivity. Low phenol selectivity strongly resulted due to repolymerization of intermediate radicals and ions of pyrolysis vapors that results in aromatic substitution side group. Thus, selective catalysts, such as vanillin, BTX, and other aromatics, are strongly required to upgrade the valued chemical production for chemistry industrial, food, pharmaceutical, and cosmetic industries.

#### Declaration of competing interest

The authors declare that they have no known competing financial interests or personal relationships that could have appeared to influence the work reported in this paper.

#### Acknowledgment

This research was supported by the National Metal and Materials Technology Center, Thailand [Project No. MT-ICF-61-POL-07-593-I].

#### References

- [1] Gillet S, Aguedo M, Petitjean L, Morais ARC, Da Costa Lopes AM, Łukasik RM, et al. Lignin transformations for high value applications: Towards targeted modifications using green chemistry. *Green Chem* 2017;19:4200–33. <http://dx.doi.org/10.1039/c7gc01479a>.
- [2] Lupoi JS, Singh S, Parthasarathi R, Simmons BA, Henry RJ. Recent innovations in analytical methods for the qualitative and quantitative assessment of lignin. *Renew Sustain Energy Rev* 2015;49:871–906. <http://dx.doi.org/10.1016/j.rser.2015.04.091>.
- [3] Zakzeski J, Bruijninx PCA, Jongerius AL, Weckhuysen BM. The catalytic valorization of lignin for the production of renewable chemicals. *Chem Rev* 2010;110:3552–99. <http://dx.doi.org/10.1021/cr900354u>.
- [4] Wang H, Pu Y, Ragauskas A, Yang B. From lignin to valuable products—strategies, challenges, and prospects. *Bioresour Technol* 2019;271:449–61. <http://dx.doi.org/10.1016/j.biortech.2018.09.072>.

- [5] Kai D, Tan MJ, Chee PL, Chua YK, Yap YL, Loh XJ. Towards lignin-based functional materials in a sustainable world. *Green Chem* 2016;18:1175–200. <http://dx.doi.org/10.1039/c5gc02616d>.
- [6] Dorrestijn E, Laarhoven LJJ, Arends IWCE, Mulder P. Occurrence and reactivity of phenoxyl linkages in lignin and low rank coal. *J Anal Appl Pyrolysis* 2000;54:153–92. [http://dx.doi.org/10.1016/S0165-2370\(99\)00082-0](http://dx.doi.org/10.1016/S0165-2370(99)00082-0).
- [7] Heitner C, Dimmel D, Schmidt J. Lignin and lignans: advances in chemistry. 2010. [http://dx.doi.org/10.1016/0076-6879\(88\)61028-7](http://dx.doi.org/10.1016/0076-6879(88)61028-7).
- [8] Funaoka M. Lignin: its functions and successive flow. *Macromol Symp* 2003;201:213–22. <http://dx.doi.org/10.1002/masy.200351124>.
- [9] Passauer L, Struch M, Schults S, Appelt J, Schneider Y, Jaros D, et al. Dynamic moisture sorption characteristics of xerogels from water-swellaable oligo(oxyethylene) lignin derivatives. *ACS Appl Mater Interfaces* 2012;4:5852–62. <http://dx.doi.org/10.1021/am3015179>.
- [10] Lan W, Luterbacher JS. A road to profitability from lignin via the production of bioactive molecules. *ACS Cent Sci* 2019;5:1642–4. <http://dx.doi.org/10.1021/acscentsci.9b00954>.
- [11] Kumar A, Anushree, Kumar J, Bhaskar T. Utilization of lignin: A sustainable and eco-friendly approach. *J Energy Inst* 2020;93:235–71. <http://dx.doi.org/10.1016/j.joei.2019.03.005>.
- [12] Zevallos Torres LA, Lorenci Woiciechowski A, de Andrade Tanobe VO, Karp SG, Guimarães Lorenci LC, Faulds C, et al. Lignin as a potential source of high-added value compounds: A review. *J Clean Prod* 2020;263:121499. <http://dx.doi.org/10.1016/j.jclepro.2020.121499>.
- [13] Diehl BG, Brown NR, Frantz CW, Lumadue MR, Cannon F. Effects of pyrolysis temperature on the chemical composition of refined softwood and hardwood lignins. *Carbon N Y* 2013;60:531–7. <http://dx.doi.org/10.1016/j.carbon.2013.04.087>.
- [14] Pandey MP, Kim CS. Lignin depolymerization and conversion: A review of thermochemical methods. *Chem Eng Technol* 2011;34:29–41. <http://dx.doi.org/10.1002/ceat.201000270>.
- [15] Son D, Gu S, Choi JW, Suh DJ, Jae J, Choi J, et al. Production of phenolic hydrocarbons from organosolv lignin and lignocellulose feedstocks of hardwood, softwood, grass and agricultural waste. *J Ind Eng Chem* 2019;69:304–14. <http://dx.doi.org/10.1016/j.jiec.2018.09.009>.
- [16] Huang Y, Wei Z, Qiu Z, Yin X, Wu C. Study on structure and pyrolysis behavior of lignin derived from corncob acid hydrolysis residue. *J Anal Appl Pyrolysis* 2012;93:153–9. <http://dx.doi.org/10.1016/j.jaap.2011.10.011>.
- [17] Kim JY, Oh S, Hwang H, Kim UJ, Choi JW. Structural features and thermal degradation properties of various lignin macromolecules obtained from poplar wood (*Populus albaglandulosa*). *Polym Degrad Stab* 2013;98:1671–8. <http://dx.doi.org/10.1016/j.polymdegradstab.2013.06.008>.
- [18] Chen L, Ye X, Luo F, Shao J, Lu Q, Fang Y, et al. Pyrolysis mechanism of  $\beta-O-4$  type lignin model dimer. *J Anal Appl Pyrolysis* 2015;115:103–11. <http://dx.doi.org/10.1016/j.jaap.2015.07.009>.
- [19] Vichaphund S, Sricharoenchaikul V, Atong D. Selective aromatic formation from catalytic fast pyrolysis of Jatropha residues using ZSM-5 prepared by microwave-assisted synthesis. *J Anal Appl Pyrolysis* 2019;141:104628. <http://dx.doi.org/10.1016/j.jaap.2019.104628>.
- [20] Park S, Jae J, Farooq A, Kwon EE, Park ED, Ha JM, et al. Continuous pyrolysis of organosolv lignin and application of biochar on gasification of high density polyethylene. *Appl Energy* 2019;255:113801. <http://dx.doi.org/10.1016/j.apenergy.2019.113801>.
- [21] Naron DR, Collard FX, Tyhoda L, Görgens JF. Production of phenols from pyrolysis of sugarcane bagasse lignin: Catalyst screening using thermogravimetric analysis – Thermal desorption – Gas chromatography – Mass spectroscopy. *J Anal Appl Pyrolysis* 2019;138:120–31. <http://dx.doi.org/10.1016/j.jaap.2018.12.015>.
- [22] Wang G, Li W, Li B, Chen H. TG study on pyrolysis of biomass and its three components under syngas. *Fuel* 2008;87:552–8. <http://dx.doi.org/10.1016/j.fuel.2007.02.032>.
- [23] Tejado A, Peña C, Labidi J, Echeverria JM, Mondragon I. Physico-chemical characterization of lignins from different sources for use in phenol-formaldehyde resin synthesis. *Bioresour Technol* 2007;98:1655–63. <http://dx.doi.org/10.1016/j.biortech.2006.05.042>.
- [24] Gellerstedt G, Lindfors EL. Structural changes in lignin during kraft pulping. *Holzforschung* 1984;38:151–8. <http://dx.doi.org/10.1515/hfsg.1984.38.3.151>.
- [25] Ramakoti B, Dhanagopal H, Deepa K, Rajesh M, Ramaswamy S, Tamilarasan K. Solvent fractionation of organosolv lignin to improve lignin homogeneity: Structural characterization. *Bioresour Technol* 2019;7:100293. <http://dx.doi.org/10.1016/j.biteb.2019.100293>.
- [26] Bu L, Tang Y, Gao Y, Jian H, Jiang J. Comparative characterization of milled wood lignin from furfural residues and corncob. *Chem Eng J* 2011;175:176–84. <http://dx.doi.org/10.1016/j.cej.2011.09.091>.
- [27] Xu F, Sun R-C, Zhai M-Z, Sun J-X, Jiang J-X, Zhao G-J. Comparative study of three lignin fractions isolated from mild ball-milled *Tamarix austromogoliac* and *Caragana sepium*. *J Appl Polym Sci* 2008;108:1158–68. <http://dx.doi.org/10.1002/app.27761>.
- [28] Brebu M, Tamminen T, Spiridon I. Thermal degradation of various lignins by TG-MS/FTIR and Py-GC-MS. *J Anal Appl Pyrolysis* 2013;104:531–9. <http://dx.doi.org/10.1016/j.jaap.2013.05.016>.
- [29] Liu JY, Wu SBin, Lou R. Chemical structure and pyrolysis response of  $\beta-O-4$  lignin model polymer. *BioResources* 2011;6:1079–93. <http://dx.doi.org/10.15376/biores.6.2.1079-1093>.
- [30] Kawamoto H, Horigoshi S, Saka S. Pyrolysis reactions of various lignin model dimers. *J Wood Sci* 2007;53:168–74. <http://dx.doi.org/10.1007/s10086-006-0834-z>.
- [31] Gu X, Ma X, Li L, Liu C, Cheng K, Li Z. Pyrolysis of poplar wood sawdust by TG-FTIR and Py-GC/MS. *J Anal Appl Pyrolysis* 2013;102:16–23. <http://dx.doi.org/10.1016/j.jaap.2013.04.009>.
- [32] Ryu HW, Lee HW, Jae J, Park YK. Catalytic pyrolysis of lignin for the production of aromatic hydrocarbons: Effect of magnesium oxide catalyst. *Energy* 2019;179:669–75. <http://dx.doi.org/10.1016/j.energy.2019.05.015>.
- [33] Lin X, Sui S, Tan S, Pittman C, Sun J, Zhang Z. Fast pyrolysis of four lignins from different isolation processes using Py-GC/MS. *Energies* 2015;8:5107–21. <http://dx.doi.org/10.3390/en8065107>.
- [34] Lou R, Wu SBin, Dong HL, Lü GJ. Fast pyrolysis of enzymatic/mild acidolysis lignin from moso bamboo. *Ranliao Huaxue Xuebao/J Fuel Chem Technol* 2015;43:42–7.

- [35] Kawamoto H. Lignin pyrolysis reactions. *J Wood Sci* 2017;63:117–32. <http://dx.doi.org/10.1007/s10086-016-1606-z>.
- [36] Dumitrache A, Akinosho H, Rodriguez M, Meng X, Yoo CG, Natzke J, et al. Consolidated bioprocessing of *Populus* using *Clostridium (ruminiclostridium) thermocellum*: A case study on the impact of lignin composition and structure. *Biotechnol Biofuels* 2016;9. <http://dx.doi.org/10.1186/s13068-016-0445-x>.
- [37] Yoo CG, Dumitrache A, Muchero W, Natzke J, Akinosho H, Li M, et al. Significance of lignin S/G ratio in biomass recalcitrance of *Populus trichocarpa* variants for bioethanol production. *ACS Sustain Chem Eng* 2018;6:2162–8. <http://dx.doi.org/10.1021/acssuschemeng.7b03586>.
- [38] Harman-Ware AE, Crocker M, Kaur AP, Meier MS, Kato D, Lynn B. Pyrolysis-GC/MS of sinapyl and coniferyl alcohol. *J Anal Appl Pyrolysis* 2013;99:161–9. <http://dx.doi.org/10.1016/j.jaap.2012.10.001>.
- [39] Asmadi M, Kawamoto H, Saka S. Thermal reactions of guaiacol and syringol as lignin model aromatic nuclei. *J Anal Appl Pyrolysis* 2011;92:88–98. <http://dx.doi.org/10.1016/j.jaap.2011.04.011>.
- [40] Chen S, Cheng H, Wu S. Pyrolysis characteristics and volatiles formation rule of organic solvent fractionized kraft lignin. *Fuel* 2020;270:117520. <http://dx.doi.org/10.1016/j.fuel.2020.117520>.
- [41] Shen D, Liu G, Zhao J, Xue J, Guan S, Xiao R. Thermo-chemical conversion of lignin to aromatic compounds: Effect of lignin source and reaction temperature. *J Anal Appl Pyrolysis* 2015;112:56–65. <http://dx.doi.org/10.1016/j.jaap.2015.02.022>.
- [42] Liu C, Hu J, Zhang H, Xiao R. Thermal conversion of lignin to phenols: Relevance between chemical structure and pyrolysis behaviors. *Fuel* 2016;182:864–70. <http://dx.doi.org/10.1016/j.fuel.2016.05.104>.
- [43] Du FL, Du QS, Dai J, Tang PD, Li YM, Long SY, et al. A comparative study for the organic byproducts from hydrothermal carbonizations of sugarcane bagasse and its bio-refined components cellulose and lignin. *PLoS One* 2018;13. <http://dx.doi.org/10.1371/journal.pone.0197188>.
- [44] Cao Y, Chen SS, Zhang S, Ok YS, Matsagar BM, Wu KCW, et al. Advances in lignin valorization towards bio-based chemicals and fuels: Lignin biorefinery. *Bioresour Technol* 2019;291:121878. <http://dx.doi.org/10.1016/j.biortech.2019.121878>.
- [45] Fache M, Boutevin B, Caillol S. Vanillin production from lignin and its use as a renewable chemical. *ACS Sustain Chem Eng* 2016;4:35–46. <http://dx.doi.org/10.1021/acssuschemeng.5b01344>.
- [46] Rodrigues Pinto PC, Borges Da Silva EA, Rodrigues AE. Lignin as source of fine chemicals: Vanillin and syringaldehyde. In: *Biomass convers. interface biotechnol. chem. mater. sci.*. Springer-Verlag Berlin Heidelberg; 2012, p. 381–420. [http://dx.doi.org/10.1007/978-3-642-28418-2\\_12](http://dx.doi.org/10.1007/978-3-642-28418-2_12).
- [47] Kotake T, Kawamoto H, Saka S. Mechanisms for the formation of monomers and oligomers during the pyrolysis of a softwood lignin. *J Anal Appl Pyrolysis* 2014;105:309–16. <http://dx.doi.org/10.1016/j.jaap.2013.11.018>.
- [48] Dorrestijn E, Mulder P. The radical-induced decomposition of 2-methoxyphenol. *J Chem Soc Perkin Trans 2* 1999;777–80. <http://dx.doi.org/10.1039/a809619h>.
- [49] Chang SJ, Hum GP, McMillen DF, Malhotra R. Hydrogen-transfer-promoted bond scission initiated by coal fragments. *Energy Fuels* 1987;1:193–8. <http://dx.doi.org/10.1021/ef00002a009>.
- [50] McMillen DF, Malhotra R, Chang SJ, Ogier WC, Nigenda SE, Fleming RH. Mechanisms of hydrogen transfer and bond scission of strongly bonded coal structures in donor-solvent systems. *Fuel* 1987;66:1611–20. [http://dx.doi.org/10.1016/0016-2361\(87\)90351-6](http://dx.doi.org/10.1016/0016-2361(87)90351-6).
- [51] Fan L, Ruan R, Li J, Ma L, Wang C, Zhou W. Aromatics production from fast co-pyrolysis of lignin and waste cooking oil catalyzed by HZSM-5 zeolite. *Appl Energy* 2020;263:114629. <http://dx.doi.org/10.1016/j.apenergy.2020.114629>.